



Single-multicomponent biosorption of lead mercury chromium and arsenic onto activated sludge in batch and fixed-bed adsorber

Abbas H. Sulaymon^a, Saib A. Yousif^{b,*}, Mustafa M. Al-Faize^b

^aPower Engineering Department, College of Engineering, University of Baghdad, Baghdad, Iraq

^bChemical Engineering Department, College of Engineering, University of Basrah, P.O. Box 1458, Basrah, Iraq

Tel. +96 47801469067; email: saib60@yahoo.com

Received 28 June 2013; Accepted 28 November 2013

ABSTRACT

A wide range of batch experiments were carried out for estimation of the key process parameters in competitive biosorption of Pb^{2+} , Hg^{2+} , Cr^{3+} , and As^{5+} from simulated of wastewater onto dry activated sludge in batch adsorber. Eleven isotherm models were used for single component and five isotherm models for multicomponent systems. The Langmuir model gave the best fit for the data of single component, while the binary, ternary, and quaternary systems were fitted successfully with extended Langmuir model. An order of metal biosorption capacity onto dried activated sludge was found to be $Pb^{2+} > Hg^{2+} > Cr^{3+} > As^{5+}$. FTIR analysis was carried out before and after biosorption. Pore diffusion coefficients required for fixed-bed design were determined by matching batch experimental data with the film-pore diffusion model at optimum agitation speed, 600 rpm and optimum weight of sewage sludge biomass. A general multicomponent rate model has been utilized to predict the fixed-bed breakthrough curves for multicomponent systems. Good agreement between the predicted theoretical breakthrough curves and the experimental results was observed. Results confirmed, from the feed containing Pb^{2+} , Hg^{2+} , Cr^{3+} , and As^{5+} , arsenic breakthrough from the column appeared first with higher overshoot, followed by chromium, mercury, and finally lead cations with no overshoot. COMSOL multiphysics software was used to solve the batch and fixed-bed models.

Keywords: Activated sludge; Batch; Fixed-bed adsorber; Multicomponent system; COMSOL software

1. Introduction

The presence of heavy metal ions in the environment has been a matter of major concern due to their toxicity to human life. Heavy metals are major

pollutants in marine, ground water, industrial, and even treated wastewater [1]. Industrial wastewater resulting from the petroleum industries and industrial activities represent the main source of environmental pollution with heavy metals. Their effects may increase nowadays because of the progressive in the industrial technologies and increasing the demand for petroleum and oil globally, thus, result in continuous

*Corresponding author.

increase of pollution. Among the toxic heavy metals, lead, mercury, chromium, and arsenic are classified as priority pollutants due to their major impact on the human life and environment.

A number of physicochemical methods have been developed over the years to remove toxic metal ions from aqueous solution which includes chelation extraction, chemical coagulation, evaporation, adsorption, extraction, chemical precipitation, ion exchange, electrochemical processes, flotation, flocculation, and membrane processes. However, the applications of such processes are sometimes restricted because of technical or economic constraints [2].

Sewage sludge is a biomass waste containing mainly bacteria and protozoa is generated from the regular biological activities of municipal wastewater treatment plants. The volume being produced is likely to increase with increase in treated municipal wastewater. Sludge treatment/disposal represents 50% of the capital and operational costs of a wastewater treatment plant. Rather than simply disposing of the sludge, considered use of this waste material seems to be a promising way of turning it into a resource. One application that has received increasing attention is the utilization of sewage sludge as abundant low-cost alternative adsorbent for the removal of pollutants from wastewater [3].

Actual wastewater treatment systems often have to deal with a mixture of heavy metals; most research work still only focuses on a single and binary metal sorption. Only a few works on the biosorption of three or more of heavy metals were found in literature. For instance, Kusvuran et al. [4] investigated the multi-metal biosorption of Cu^{2+} , Cd^{2+} , and Pb^{2+} from real industrial water and contaminated water using waste activated sludge biomass and reported that the adsorption capacity of activated sludge biomass was observed in the order of $\text{Cu}^{2+} > \text{Cd}^{2+} > \text{Pb}^{2+}$.

The aim of this study was to investigate the sorption capacity and to evaluate the performance of dry activated sludge (DAS) batch and fixed-bed systems for the removal of Pb^{2+} , Hg^{2+} , Cr^{3+} , and As^{5+} in single, binary, ternary, and quaternary systems from simulated wastewater.

2. Mathematical model

2.1. Batch adsorber

The overall rate of biosorption in a porous biosorbent can be described by a mechanism of three consecutive steps: (1) external mass transport, (2) intraparticle diffusion, and (3) adsorption at an

interior site. Moreover, intraparticle diffusion may be governed by pore volume diffusion or surface diffusion or a combination of both. For batch adsorber, the mathematical model with pore diffusion model [5] is:

- Mass balance in fluid-bulk phase:

$$V_L \frac{dC_b}{dt} + \frac{3W_A}{\rho_p R_p} k_f (C_b - C_{p,r=R_p}) = 0 \quad (1)$$

- Mass balance inside particle phase:

$$\varepsilon_p \frac{\partial C_p}{\partial t} + \rho_p \frac{\partial q}{\partial t} = \varepsilon_p D_p \frac{1}{R^2} \frac{\partial}{\partial R} \left(R^2 \frac{\partial C_p}{\partial R} \right) \quad (2)$$

- Initial and boundary conditions:

$$t = 0; C_b = C_o, C_p = 0, q = 0$$

$$R = 0; \left(\frac{\partial C_p}{\partial R} \right)_{R=0} = 0 \quad \left(\frac{dq}{dR} \right)_{R=0} = 0$$

$$R = R_p; \varepsilon_p D_p \left(\frac{\partial C_p}{\partial R} \right)_{R=R_p} = k_f [C_b - C_{p,R=R_p}]$$

In case of applying Langmuir isotherm model [6]:

$$q = \frac{q_m b C_p}{1 + b C_p} \quad (3)$$

For scaled bulk concentration, $C'_b = C_b/C_o$, Eq. (1) becomes:

$$V_L \frac{dC'_b}{dt} + \frac{3W_A k_f}{\rho_p R_p} (C'_b - C'_{p,r=R_p}) = 0 \quad (4)$$

For scaled particle phase concentration, $C'_p = C_p/C_o$, and taking into account that,

$$\frac{\partial q}{\partial t} = \frac{\partial q}{\partial C'_p} \cdot \frac{\partial C'_p}{\partial t}$$

$$\text{where } \frac{\partial q}{\partial C'_p} = \frac{q_m b}{(1 + b C_o C'_p)^2}$$

Eq. (2) becomes:

$$\left[\varepsilon_p + \frac{\rho_p q_m b}{(1 + b C'_p C_0)^2} \right] \frac{\partial C'_p}{\partial t} = \varepsilon_p D_p \frac{\partial^2 C'_p}{\partial t^2} + \frac{2 \varepsilon_p D_p}{R} \frac{\partial C'_p}{\partial R} \quad (5)$$

With the scaled initial and boundary conditions,

$$t = 0; C'_b = 1, C'_p = 0, q = 0 \quad (6)$$

$$R = 0; \left(\frac{\partial C'_p}{\partial R} \right) = 0 \quad (7)$$

$$R = R_p; \varepsilon_p D_p \left(\frac{\partial C'_p}{\partial R} \right)_{r=R_p} = k_f [C'_b - C'_{p,R=R_p}] \quad (8)$$

An external mass transfer coefficient for the solute adsorbed at certain particle size and optimum agitation speed, can be obtained by the analytical solution of Eq. (1) [7], where at $t = 0, C_{p,r=R_p} = 0$ and $C_b = 0$, hence,

$$k_f = - \frac{R_p \rho_p V_L}{3 W t} \ln \left(\frac{C_b}{C_0} \right) \quad (9)$$

where t is the sampling time period.

2.2. Fixed-bed adsorber

A general multicomponent rate model (GMRM) used in this study takes into account axial dispersion, external mass transfer, interparticle diffusion, and nonlinear adsorption isotherm [8]. The model governing equations for component i are:

- Continuity equation in the bulk-fluid phase:

$$\frac{\partial C_{bi}}{\partial t} = -v \frac{\partial C_{bi}}{\partial z} + D_L \frac{\partial^2 C_{bi}}{\partial z^2} - \frac{(1 - \varepsilon_b)}{\varepsilon_b} \rho_p \frac{\partial q_i}{\partial t} \quad (10)$$

For film diffusion, the sorption term $\frac{\partial q_i}{\partial t}$ is given by,

$$\frac{\partial q_i}{\partial t} = \frac{3 k_{fi}}{R_p \rho_p} (C_{bi} - C_{pi,R=R_p}) \quad (11)$$

Substituting the film diffusion expression back into Eq. (10) and rearranging yields:

$$- D_L \frac{\partial^2 C_{bi}}{\partial z^2} + v \frac{\partial C_{bi}}{\partial z} + \frac{\partial C_{bi}}{\partial t} + \frac{3 k_{fi} (1 - \varepsilon_b)}{\varepsilon_b R_p} [C_{bi} - C_{pi,R=R_p}] = 0 \quad (12)$$

- Continuity equation inside the macropores.

The intraparticle mass balance in the radial direction in spherical coordinates accounting for pore diffusion is:

$$\varepsilon_p \frac{\partial C_{pi}}{\partial t} + (1 - \varepsilon_p) \rho_p \frac{\partial q_i}{\partial t} - \varepsilon_p D_{pi} \left[\frac{1}{R^2} \frac{\partial}{\partial R} \left(R^2 \frac{\partial C_{pi}}{\partial R} \right) \right] = 0 \quad (13)$$

- Initial and boundary conditions:

$$C_{bi} = C_{bi}(0, z) = 0 \quad (14)$$

$$C_{pi} = C_{pi}(0, R, z) = 0 \quad (15)$$

$$z = 0: \frac{\partial C_{bi}}{\partial z} = \frac{v}{D_L} (C_{bi} - C_{oi}) \quad (16)$$

$$z = L: \frac{\partial C_{bi}}{\partial z} = 0 \quad (17)$$

$$R = 0: \frac{\partial C_{pi}}{\partial R} = 0 \quad (18)$$

$$R = R_p: \frac{\partial C_{pi}}{\partial R} = \frac{k_{fi}}{\varepsilon_p D_{pi}} (C_{bi} - C_{pi,R=R_p}) \quad (19)$$

The scaled bulk concentration, c_{bi} , scaled intraparticle concentration, c_{pi} , and scaled particle dimension are defined as followed,

$$c_{bi} = \frac{C_{bi}}{C_{oi}}, c_{pi} = \frac{C_{pi}}{C_{oi}}, r = \frac{R}{R_p}$$

In case of applying extended Langmuir isotherm model for multicomponent systems [6] in which metal uptake, q_i is related to the scaled intraparticle concentration, c_{pi}

$$q_i = \frac{q_{mi} b_i C_{oi} c_{pi}}{1 + \sum_{j=1}^N b_j C_{oi} c_{pj}} \quad (20)$$

and taking into account that,

$$\frac{\partial q_i}{\partial t} = \frac{\partial q_i}{\partial c_{pi}} \cdot \frac{\partial c_{pi}}{\partial t} \quad (21)$$

where

$$\frac{\partial q_i}{\partial c_{pi}} = \frac{q_{mi} b_i \left(1 + \sum_{\substack{j=1 \\ j \neq i}}^N b_j C_{oj} c_{pj} \right)}{\left(1 + \sum_{j=1}^N b_j C_{oj} c_{pj} \right)^2} \quad (22)$$

The model Eqs. (12) and (13) can be transformed into the following semi-dimensionless equations:

$$-D_L \frac{\partial^2 c_{bi}}{\partial z^2} + v \frac{\partial c_{bi}}{\partial z} + \frac{\partial c_{bi}}{\partial t} + \frac{3k_{fi}(1 - \varepsilon_b)}{\varepsilon_b R_p} [c_{bi} - c_{pi, R=R_p}] = 0 \quad (23)$$

$$\left[\varepsilon_p + (1 - \varepsilon_p) \rho_p \frac{\partial q_i}{\partial c_{pi}} \right] \frac{\partial c_{pi}}{\partial t} = \frac{\varepsilon_p D_{pi}}{R_p^2} \frac{\partial^2 c_{pi}}{\partial r^2} + \frac{2\varepsilon_p D_{pi}}{R_p^2 r} \frac{\partial c_{pi}}{\partial r} \quad (24)$$

Initial and boundary conditions become;

$$c_{bi} = c_{bi}(0, z) = 0 \quad (25)$$

$$c_{pi} = c_{pi}(0, r, z) = 0 \quad (26)$$

$$z = 0: \frac{\partial c_{bi}}{\partial z} = \frac{v}{D_L} (c_{bi} - c_{oi}) \quad (27)$$

$$z = L: \frac{\partial c_{bi}}{\partial z} = 0 \quad (28)$$

$$r = 0: \frac{\partial c_{pi}}{\partial r} = 0 \quad (29)$$

$$r = 1: \frac{\partial c_{pi}}{\partial r} = \frac{R_p k_{fi}}{\varepsilon_p D_{pi}} (c_{bi} - c_{pi, R=R_p}) \quad (30)$$

3. Experimental work and procedure

3.1. Dry activated sludge

Activated sludge was used as a biosorbent in the present work. It was obtained from aerobic secondary unit in Hamdan wastewater treatment station in Basrah city, Iraq. The sludge was washed several times with distilled water to remove undesired solid materials and dissolved heavy metals, dried under

sun light, and then dried in oven at 60°C until having constant weight (24 h). The dry sludge was crushed by jaw crusher (Retsch, type-BB1A, Germany) and sieved by successive sieves (Retsch, ASTM-E11, Germany). Four particle sizes were obtained, 0.206, 0.380, 0.516, and 0.778 mm. The physicochemical and biological properties of DAS biomass were listed in Table 1.

3.2. Adsorbate

The stock solution of 1,000 mg/L of each metal ions of Pb(II), Hg(II), Cr(III), and As(V) were prepared by dissolving Pb(NO₃)₂, Hg(NO₃)₂·1/2H₂O, Cr(NO₃)₃·9H₂O and 3As₂O₅·5H₂O salts, respectively, in distilled water, then stored in acid washed polyethylene and glass containers and kept in refrigerator. Solutions of ions concentration of 50 mg/L were prepared by dilution of stock solution. The chemicals used are of annular grade produced by Fluka, Switzerland and BDH, UK.

3.3. Procedure

The effect of pH on biosorption of Pb²⁺, Hg²⁺, Hg²⁺, and As⁵⁺ onto DAS was investigated. A sample of (100 mL) of each single-metal ion solution was

Table 1
Physicochemical and biological properties of DAS

Biomass			
Physical characteristic		Biological characteristic	CFU/ mL
Particle density, kg/m ³	1,968	Bacteria	
Bulk density, kg/m ³	784.34	<i>Aeromonas</i> sp.	222,000
Specific surface area, m ² /g	6.999	<i>Escherichia coli</i>	430,000
pH	7.3	<i>Pseudomonas aeruginosa</i>	703,500
Bed voidage	0.601	<i>Klebsiella</i> sp.	210,000
Particle porosity	0.76	<i>Clostridium</i>	370,000
Ash content%	12	<i>Staphylococcus</i> sp.	210,000
CEC, meq/100 g	51.153	<i>Streptococcus</i> sp.	490,000
		<i>Salmonella</i> sp.	190,000
		<i>Shigella dysentery</i>	410,000
		Fungi	
		<i>Penicillium</i> sp.	180,000
		Yeast	
		<i>Candida albicans</i>	460,000
		Protozoa	
		<i>Entamoeba</i> sp.	16,000
		<i>Giardia lamblia</i>	90,000

CEC—cation exchange capacity.

CFU—colony-forming unit.

placed in a beaker of (200 mL). The solution was agitated (constant temperature 25°C) at 800 rpm. Activated sludge of weight 0.25 g and size 0.38 mm was added gradually. The solution pH was maintained at different values ranging from 2 to 7 by adding (0.5 N) HCl or NaOH to each solution and measuring the pH value continuously till reaching the desired value. After 4–7 h of agitation, the solution was filtrated using filter paper type (Wattmann No. 4) and a sample of (2 mL) was taken for analysis. An ion concentration in the supernatant was measured using atomic absorption spectrophotometer (model VGP-210 Buck scientific, USA) at 283.3, 253.7, 357.9, and 193.7 nm wavelengths for lead, mercury, chromium, and arsenic metals, respectively.

For the determination of equilibrium biosorption isotherm, the same above procedure was performed. The pH was kept at optimum value in each run. Different weights of activated sludge (0.0625, 0.125, 0.25, 0.375, 0.5, 1, 1.5, 2, 2.5, 3, 4, and 5 g) were used for each metal ions isotherm. The adsorbed amount was calculated using the following mass balance equation:

$$q_e = \frac{(V_L C_o - V_f C_e)}{W} \quad (31)$$

To determine optimum agitation speed, a wide range of speeds were performed 200, 400, 600, and 800 rpm. A (250 mL) beaker was used and an adjustable speed mixer was connected to this beaker, the beaker was filled with (100 mL) at the same initial concentration of (50 mg/L) for each solution. A mass of (2 g) of activated sludge was used in lead and mercury solutions in each experiment. While for chromium, the mass is 3 g and 4 g for arsenic solution of activated

sludge used in each experiment. A sample was then taken at (15, 30, 60, 120, 180, and 240 min) and a decay curve was plotted for (C_b/C_o) against time and as soon as (C_b/C_o) reaches (0.05), this speed of agitation considered as an optimum speed.

The optimum activated sludge weight for each pollutant was determined according to the optimum agitation speed. The optimum activated sludge weight to reach equilibrium concentration of $C_e/C_o = 0.05$ was calculated from isotherm equation for each solute.

The external mass transfer coefficient (k_f) was determined from the concentration decay curves data at optimum sludge dosage and optimum agitation speed using Eq. (9). A 2000 mL Pyrex beaker was used which is fitted with electrical mixer with glass impeller. The beaker was filled with 1,000 mL of (50 mg/L) pollutant initial concentration and the agitation speed is adjusted on (600 rpm) as an optimum speed. At time zero, samples of (2 mL) were taken after (2, 4, 6, 8, and 10 min) during the experiment for analysis.

The functional groups of activated sludge were detected by FTIR analysis before and after biosorption. The proportion of activated sludge biomass/KBr is 1/100. The background was obtained from the scan of pure KBr (Shimadzu-S1394, spectrum system, Japan) was used for FTIR analysis of DAS.

The fixed-bed experiments were carried out in Perspex glass column of 50 mm (I.D.) and 50 cm in height with perforated support at the bottom of the column to support the activated sludge bed and distributor at the top of the column. Bed height was fixed at 5 cm. Plastic Raschig rings were placed at the top of the activated sludge bed to ensure a uniform distribution of the influent through the biosorbent bed. Feed solution at 50 mg/L metal ions concentrations was prepared in 30-liter feed tank and introduced to

Table 2
COMSOL software steps and settings

Step	Description	Batch system	Fixed bed
1	Generating of the geometry	1D-particle	1D-column 2D-particle
2	Definition of physical laws	$\delta_{ts} \frac{\partial C_p}{\partial t} + \nabla \cdot (-D \nabla C_p) = R$	$\delta_{ts} \frac{\partial C_b}{\partial t} + \nabla \cdot (-D \nabla C_b) = R - u \nabla C_b$ $\delta_{ts} \frac{\partial C_p}{\partial t} + \nabla \cdot (-D \nabla C_p) = R$
3	Definition of initial and boundary condition	Eqs. (6)–(8)	Eqs. (25)–(30)
4	Specifying extrusion coupling variables	–	This property was used for two domains of different dimensions e.g. column and particle
5	Mesh generation	120 node	120 node-column 3,600 node-particle
6	Running the solution	Polynomial of five degree Time dependent, $\Delta t = 0.1$ s	Polynomial of five degree Time dependent, $\Delta t = 0.1$ s

the column via a pump at flowrate $1.4 \times 10^{-6} \text{ m}^3/\text{s}$ through calibrated rotameter and distributor. The pH was adjusted throughout the runs at optimum value. Samples were taken every 10 min, the concentration of each solute in these samples were measured using atomic absorption spectrophotometer.

4. Numerical solution using COMSOL software

The numerical solution by COMSOL software [9] relies on the finite element method. The software runs the finite element analysis together with adaptive meshing and error control using a variety of numerical solvers. When setting up the model in COMSOL Multiphysics, it is important to follow six basic steps as listed in Table 2.

5. Results and discussion

5.1. Optimum pH

Fig. 1 shows the effect of pH on the biosorption capacity of dried activated sludge. As can be seen from the figure, there was an increase in biosorption capacity of biomass with increasing pH from 2.0 to 4.0. As the pH increased, the overall surface charge of the dried activated sludge became negative and adsorption increased. At pH values higher than 4.0, biosorption studies could not be performed due to the precipitation of metal hydroxide from the solution. Thus, pH of value 4 was considered as an optimum pH.

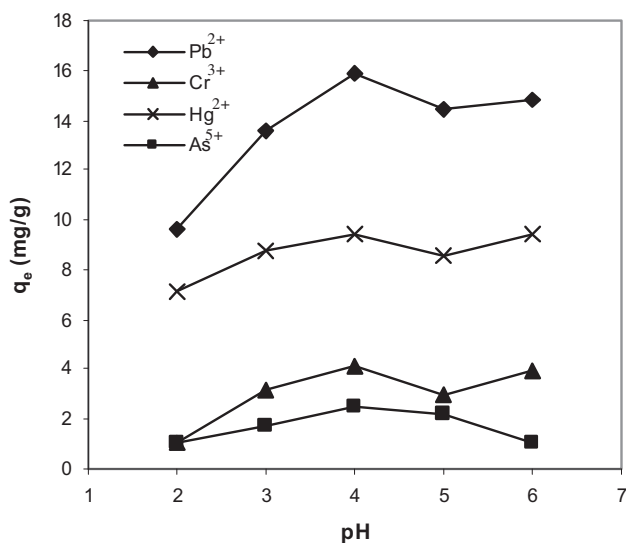


Fig. 1. Effect of pH on the uptake of Pb²⁺, Hg²⁺, Cr³⁺, and As⁵⁺ onto DAS at 298 K. $C_0 = 50 \text{ mg/L}$ for each component.

5.2. Characterization of DAS biomass

In order to find out which functional groups were responsible for the Pb²⁺, Hg²⁺, Cr³⁺, and As⁵⁺ biosorption, FTIR analysis of raw and loaded dried activated sludge was experienced before and after cations binding as listed in Table 3. The difference between the two spectra was in the absorbance wave number and intensity. Different functional groups were detected on the DAS surface. Spectra analysis of FTIR spectrum after cations absorption showed that there was a substantial decrease in the wave number and absorption intensity of carboxylic acid group with O-H stretch, amide group with N-H stretch, and amine group with N-H₂ stretch at 3411.84, 2929.81, 1652.88, 1,570, and 1,450 cm⁻¹. These groups were mainly from polysaccharide and protein materials which constitute most of the cell wall. The results show that cations may be complexed by H and O atoms of hydroxyl bonds, which shifted the bands to lower frequencies. These results agreed with [10]. According to Table 3, lead cations exhibited more decrease in wave number and absorption intensity compared to the other cations which explained its high affinity to the biosorbent.

Table 1 shows that the sewage sludge used in this work contained a much higher cation exchange capacity (51.153 meq/100 g), This indicates that CEC was an important mechanism in biosorption of Pb²⁺, Hg²⁺, Cr³⁺, and As⁵⁺ onto DAS.

Electron scanning microscopy (16 kV, Vega, Tecsan) evidenced that the sewage sludge possessed a very rough surface that could provide a large chemical binding area, Fig. 2.

5.3. Equilibrium isotherms for single component

The biosorption isotherms were obtained by plotting the weight of the solute adsorbed per unit weight of activated sludge (q_e) against the equilibrium concentration of the solute in the solution (C_e) at constant temperature. The equilibrium isotherms of Pb²⁺, Hg²⁺, Cr³⁺, and As⁵⁺, were conducted at (25°C) with initial concentration of each component, $C_0 = 50 \text{ mg/L}$. These isotherms are shown in Figs. 3–6. Eleven isotherm models were used to fit the experimental data, namely, Freundlich [11], Dubinin–Radsukevch [12], Temkin [13], Khan [14], Combination of Langmuir–Freundlich [15], Langmuir [6], Radke–Praunsitz [16], Toth [17], Reddlich–Peterson [18], Harkins–Henderson [19], and BET [20]. The values of model parameters are evaluated by nonlinear curve fitting method using DataFit version 9.0.59, Oakdale Engineering software. It is clear from Fig. 3 that the equilibrium isotherm for each single component is of favorable type, since $0 >$

Table 3
FTIR analysis for raw and loaded DAS

Functional group	Type of bond	Loaded DAS									
		Raw DAS		Pb ²⁺		Hg ²⁺		Cr ³⁺		As ⁵⁺	
		Wave no. cm ⁻¹	Tr (%) ^a	Wave no. cm ⁻¹	Tr (%)						
Carboxylic acid, Amine, Amide	O–H stretch, N–H ₂ stretch, N–H stretch	3411.84	0.21	3404.13	0.66	3411.84	0.54	3411.84	0.32	3406.05	0.38
Alkanes, Carboxylic acid	C–H stretch, O–H stretch	2925.81	0.31	2923.88	0.88	2923.88	0.8	2923.88	0.74	2923.88	0.625
Alkanes, Carboxylic acid	C–H stretch, O–H stretch	2854.45	0.55	2854.45	1.22	2854.45	1.08	2854.45	1.03	2854.45	1
Carboxylic acid, Alkenes, Amides, Imines	C=O stretch, C=C stretch, N–H stretch, R ₂ C=N–R stretch	1652.88	0.155	1647.1	0.6	1652.88	0.58	1650.95	0.6	1652.88	0.38
Amides, Nitro groups, Amines	N–H bend, NO ₂ (aliphatic), N–H ₂ bend	1,570	0.225	1,560	0.64	1,550	0.65	1,550	0.78	1,570	0.6
Amines, Amides, Nitro groups,	N–H ₂ bend, N–H bend, NO ₂ (aromatic)	1,520	0.15	1,520	0.6	—	—	—	—	1,520	0.51
Carboxylic acids	O–H bend	1,450	0.058	1440.73	0.52	1442.66	0.535	1,445	0.65	1434.94	0.4
Alkenes, Carboxylic acid,	C–H in-plane bend, C=O stretch, O–H bend	1417.5	0.058	—	—	—	—	1417.5	0.6	1417.5	0.4
Alcohols, Ethers, Carboxylic acid, Alkyl halides, phosphines	–OH stretch, C–O–C stretch, C–F stretch, P–H bend	1016.42	0.05	1016.42	0.21	1016.42	0.26	1016.42	0.2	1016.42	0.06
Sulfonates, phosphines	S–O stretch, P–H bend	873.69	0.20	873.69	0.9	873.69	0.875	873.69	1.1	873.69	0.68

^aTransmittance %, —: No peak.

$R_s < 1$ ($R_s = 0.4228, 0.0623, 0.0771,$ and 0.0862 for $Pb^{2+}, Hg^{2+}, Cr^{3+},$ and As^{5+} , respectively).

For lead; Langmuir, Radke-Praunsitz, Khan, Redlich-Peterson, and Toth gave the best fit of experimental data with high correlation coefficients ($R^2 = 0.9979$). While, the experimental data for mercury, chromium, and arsenic were described successfully with Langmuir model with correlation coefficient 0.9923, 0.9897, and 0.9868, respectively. Thus, Langmuir model was used in the modeling of batch adsorber for all of heavy metals in this study. Using Langmuir model, it was found that the maximum metal uptake (q_m) for Pb^{2+} is greater than that for $Cr^{3+}, Hg^{2+},$ and As^{5+} ($q_{m,Pb^{2+}} = 77.4857, q_{m,Hg^{2+}} = 10.7876, q_{m,Cr^{3+}} = 4.6404,$ and $q_{m,As^{5+}} = 2.8289$ mg/g, respectively). These are in agreement with other studies ($q_{m,Pb^{2+}} = 87.7, q_{m,Cr^{3+}} = 3$ mg/g) [21,22]. Higher q_m value for Pb^{2+} confirms the stronger bonding affinity of DAS to Pb^{2+} than to that of $Cr^{3+}, Hg^{2+},$ and As^{5+} .

The adsorption capacity of lead, mercury, chromium, and arsenic cations onto commercial activated carbon for other studies were $q_{m,Pb^{2+}} = 13.2608, q_{m,Hg^{2+}} = 71.4136, q_{m,Cr^{3+}} = 2.756,$ and $q_{m,As^{5+}} = 20.233$ mg/g) [23–25]. On comparing with present study, DAS

seemed poor to adsorb Hg^{2+} and As^{5+} , but its availability and low cost make it promising alternative.

5.4. Equilibrium isotherms for multicomponents systems

The biosorption equilibrium isotherms for the binary, ternary, and quaternary component systems were conducted by preparing a solution with initial concentration of (50 mg/L) for each pollutant and using DAS of size (0.38 mm). The equilibrium concentrations were measured in the presence of the other pollutant, the results are shown in Figs. 3–6. Five isotherm models were used to fit the experimental data, namely, Harkins–Jura [24], Halsey–Henderson [26], Combination of Langmuir–Freundlich [27], Redlich–Peterson [27], and extended Langmuir [6].

For the binary, ternary, and quaternary systems, the extended Langmuir model seems to give the best fitting for the experimental data i.e. highest value of (R^2). In addition, combination of Langmuir–Freundlich and Redlich–Peterson models may participate with extended Langmuir model to give the best fit for some systems. The behavior of an equilibrium isotherm was a favorable type. It can be seen from the figures, Pb^{2+}

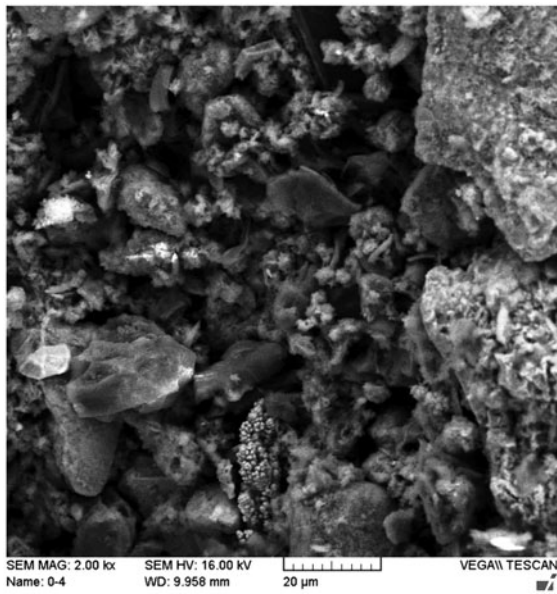


Fig. 2. SEM image of DAS shows the amorphous structures.

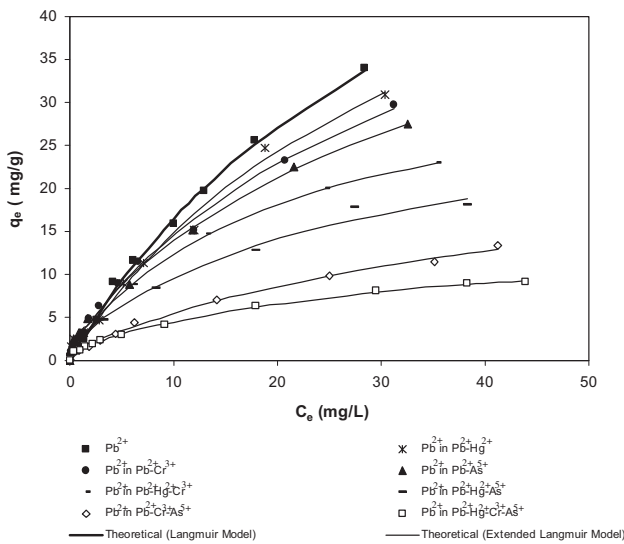


Fig. 3. Biosorption isotherm for Pb^{2+} in single, binary, ternary, and quaternary systems onto DAS at 25°C.

always adsorbed more favorably onto activated sludge than Hg^{2+} , Cr^{3+} , and As^{5+} in the binary, ternary, and quaternary systems. The results also indicate that Pb^{2+} was the metal that experienced the least displacement in the competitive adsorption process. Hg^{2+} , Cr^{3+} , and As^{5+} had little influence on the Pb^{2+} biosorption in the presence of activated sludge. Conversely, Pb^{2+} significantly inhibited the retention of Hg^{2+} , Cr^{3+} , and As^{5+} while As^{5+} was most affected in the competitive adsorption. From the figures, it is clear that at low

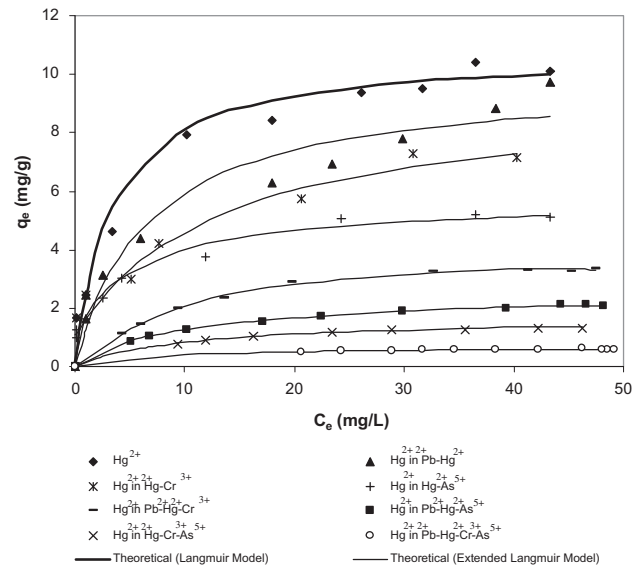


Fig. 4. Biosorption isotherm for Hg^{2+} in single, binary, ternary, and quaternary systems onto DAS at 25°C.

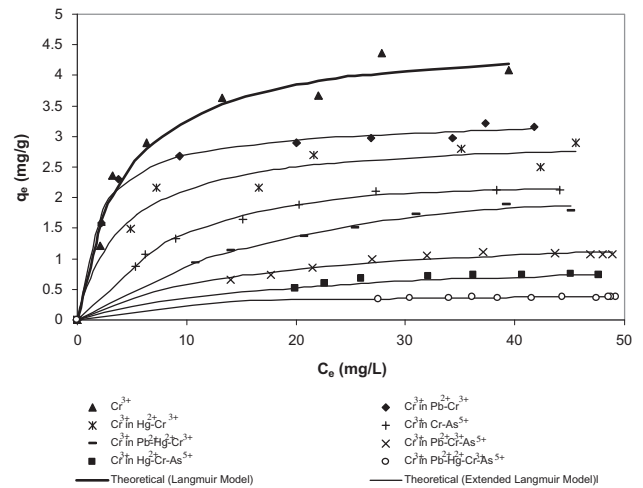


Fig. 5. Biosorption isotherm for Cr^{3+} in single, binary, ternary, and quaternary systems onto DAS at 25°C.

concentrations, the amount adsorbed for both/all metal ions increased due to the abundant biosorption sites on activated sludge. As the concentration of both/all metal ions species increased further, the adsorption sites were also available to both/all adsorbed species which were occupied to an increasing extent by the more strongly adsorbed species, resulting in a decrease in the amount of the more weakly adsorbed species. Furthermore, when metals are competing for the same type of biosorbent, metals with greater affinity (strongly adsorbed species) will displace others with a lower affinity (weakly adsorbed

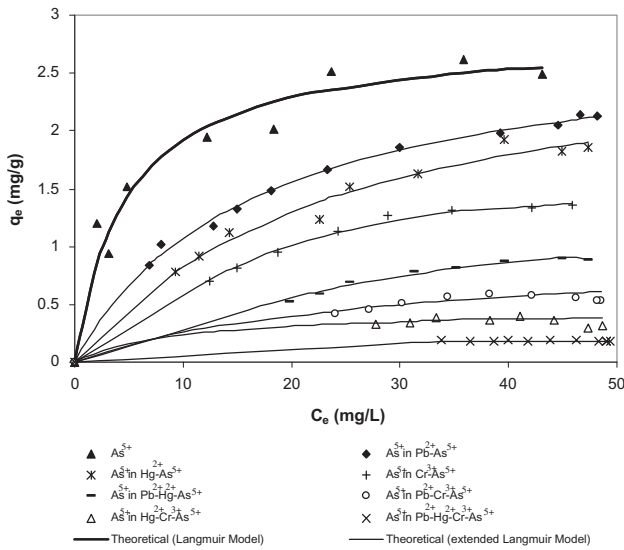


Fig. 6. Biosorption isotherm for As^{5+} in single, binary, ternary, and quaternary systems onto DAS at 25°C.

species). Among the four metal ions, As^{5+} was the weakest adsorbed ion, therefore when the stronger competitive species Pb^{2+} in solution compete with the weakest adsorbed species As^{5+} , this may undergo displacement. Compared with their sorption in single-component systems, an individual biosorption capacity of all four metals showed obvious decrease in the binary (11–51%), ternary (53–88%), and quaternary systems (79–94%). The biosorption capacity decreased more in the quaternary system as compared with binary and ternary systems. Since in a binary, ternary, and quaternary systems the vacant (unoccupied biosorption sites) will be reduce and that in turn affecting the sorption capacity in these systems.

5.5. Dynamic parameters of fixed bed

Pore diffusion coefficient D_p for each metal ions are evaluated from the concentration decay curve by matching the experimental data with the predicted data by pore diffusion model for batch adsorber as shown in Fig. 7.

There are a good matching between the batch experimental results and predicted data using pore diffusion model for batch adsorber. The pore diffusion coefficient for each of the metal ions was evaluated elsewhere [28] by minimizing the difference of experimental and predicted concentration-time decay curves and found to be:

$$\begin{aligned}
 Pb^{2+} : D_p &= 5.9030 \times 10^{-9} \text{ m}^2/\text{s} \\
 Hg^{2+} : D_p &= 3.0551 \times 10^{-9} \text{ m}^2/\text{s} \\
 Cr^{3+} : D_p &= 1.990 \times 10^{-9} \text{ m}^2/\text{s}
 \end{aligned}$$

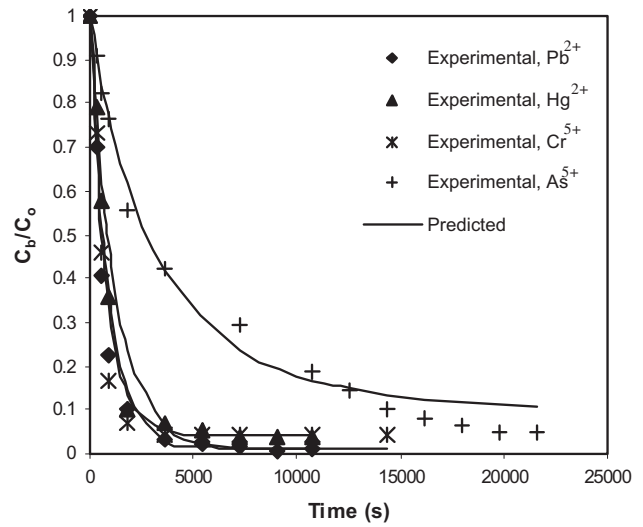


Fig. 7. Experimental and predicted concentration-time decay curves for Pb^{2+} , Hg^{2+} , Cr^{3+} , and As^{5+} .

$$As^{5+} : D_p = 1.0335 \times 10^{-9} \text{ m}^2/\text{s}$$

The optimum amount of DAS used for each metal ions was calculated for final equilibrium, related concentration of $C_e/C_o=0.05$, using the Langmuir isotherm with mass balance, Eq. (31) at optimum agitation speed which was found experimentally to be 600 rpm. These doses are 9.6939, 10.2719, 27.3703, and 48.4872 g for Pb^{2+} , Hg^{2+} , Cr^{3+} , respectively.

The external mass transfer coefficient in packed bed column model was calculated using the correlation of Wilson and Geankoplis:

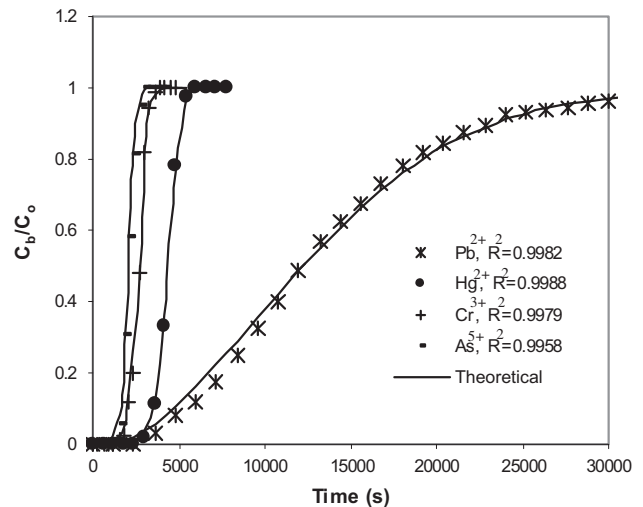


Fig. 8. Breakthrough curve for biosorption of single-heavy metal onto DAS. $C_o = 50$ mg/L each metal cations.

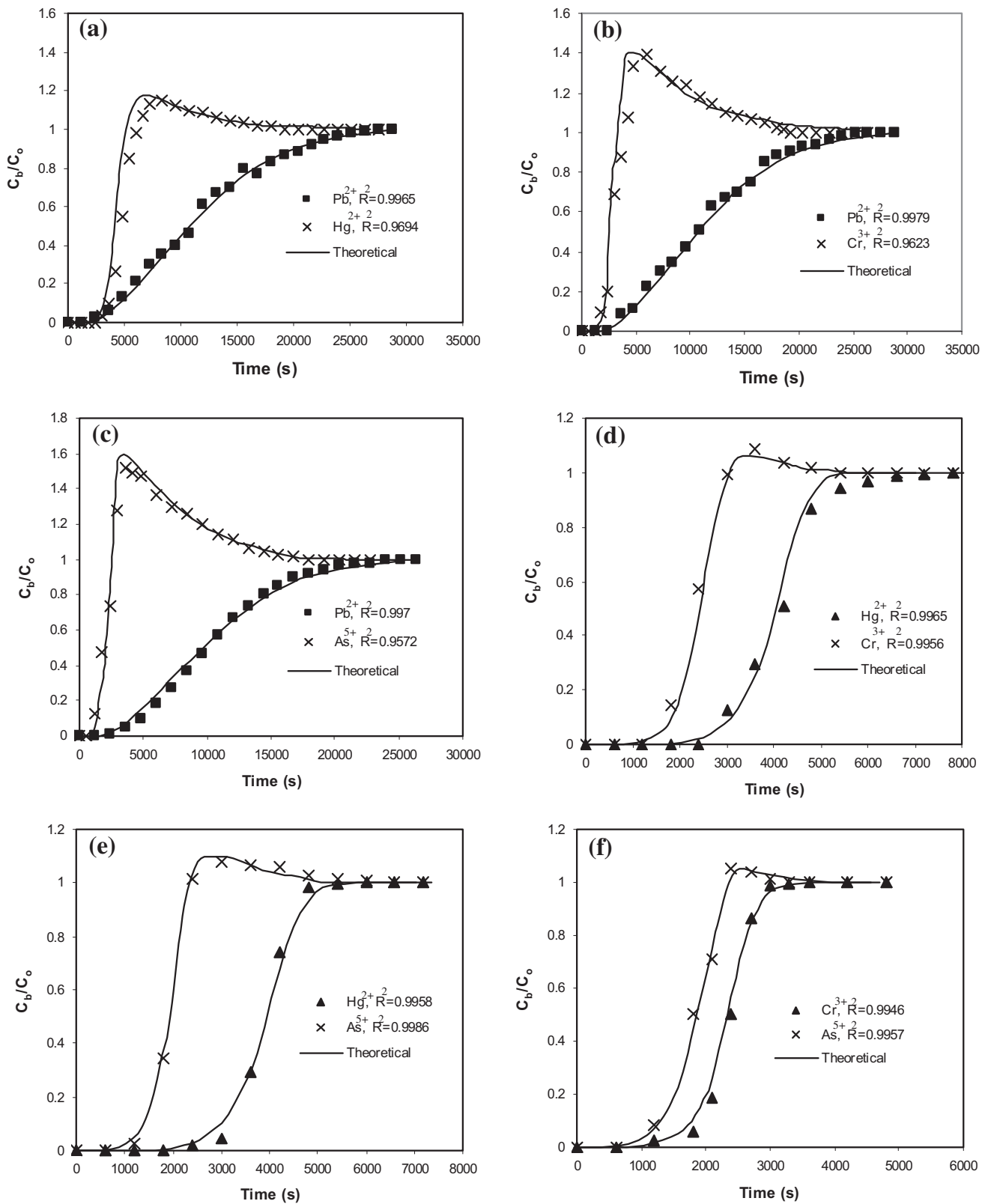


Fig. 9. Breakthrough curves for biosorption of heavy metals onto DAS in binary systems. (a) Pb^{2+} - Hg^{2+} , (b) Pb^{2+} - Cr^{3+} , (c) Pb^{2+} - As^{5+} , (d) Hg^{2+} - Cr^{3+} , (e) Hg^{2+} - As^{5+} , and (f) Cr^{3+} - As^{5+} . $C_0 = 50$ mg/L each metal cations.

$$Sh_i = \frac{1.09}{\epsilon_p} Re^{1/3} Sc_i^{1/3} \text{ for } 0.0015 < Re < 55 \quad (32)$$

The axial dispersion coefficient D_{Li} of the liquid flowing through a fixed bed was obtained from the correlation of Chung and Wen [29]:

$$D_L = \frac{Re}{(0.2 + 0.011 * Re^{0.48})} \left(\frac{\mu_w}{\rho_w} \right) \quad (33)$$

The value of liquid diffusivity coefficient (D_m) was calculated using the following equation [30]:

$$D_{m_i} = 2.74 \times 10^{-9} (MW_i)^{-1/3} \quad (34)$$

5.6. Single-component fixed-bed adsorber

The lead, mercury, chromium, and arsenic ions biosorption onto DAS in fixed-bed column as single systems at 25°C are shown in Fig. 8. The flowrate,

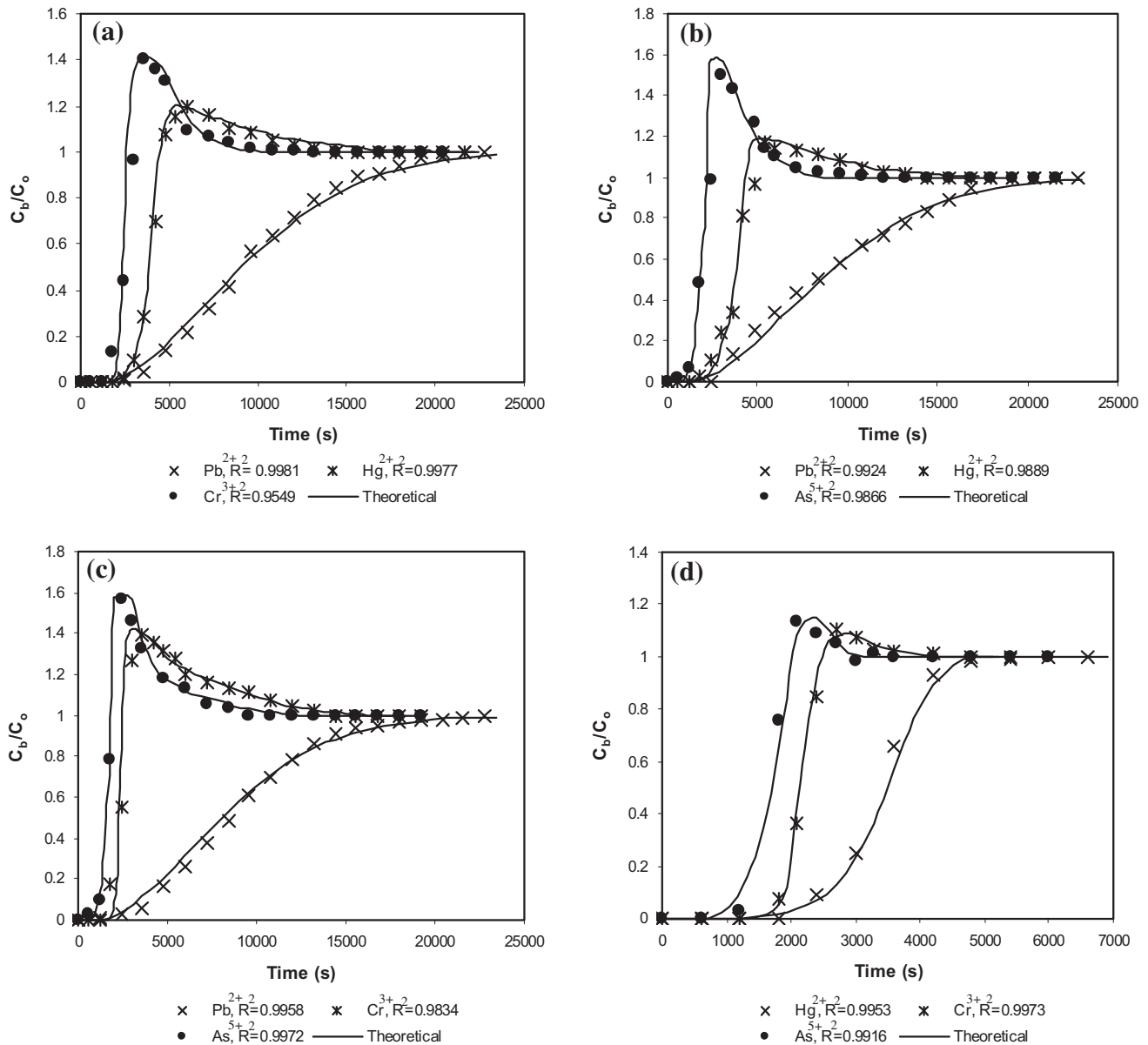


Fig. 10. Breakthrough curves for biosorption of heavy metals onto DAS in ternary systems. (a) Pb^{2+} - Hg^{2+} - Cr^{3+} , (b) Pb^{2+} - Hg^{2+} - As^{5+} , (c) Pb^{2+} - Cr^{3+} - As^{5+} , and (d) Hg^{2+} - Cr^{3+} - As^{5+} . $C_o = 50$ mg/L each metal cations.

initial metal concentration, bed height, and biosorbent particle size were $1.4 \times 10^{-6} \text{ m}^3/\text{s}$, 50 mg/L, 0.05 m, and 0.38 mm, respectively.

A comparison among the pollutants, it is clear that the breakthrough curve is more flat for Pb^{2+} and the breakpoint appears later than that for Hg^{2+} , Cr^{3+} , and As^{5+} . This confirms that lead is the strongly adsorbed component due to its highly affinity to the biosorbent and attached on the vacant sites of the adsorbent that enhancing the biosorption properties of the lead. For arsenic, the breakthrough curve is steeper and breakpoint appears early. Thus, arsenic cation is considered the weakly adsorbed component. The time for reaching breakpoint ($C_e/C_o = 0.05$) for lead, mercury, chromium, and arsenic ions were found to be 3,425, 3,115, 1810, and 1,375 s, respectively.

5.7. Multicomponent biosorption

Competitive biosorption of lead, mercury, chromium, and arsenic ions onto DAS in fixed-bed adsorber was conducted at constant operating conditions. The flowrate, initial concentration of each metal ions, bed height, biosorbent particle size, and temperature were $1.4 \times 10^{-6} \text{ m}^3/\text{s}$, 50 mg/L, 0.05 m, 0.38 mm, and 25°C, respectively. The experimental and predicted breakthrough curves for binary, ternary, and quaternary systems are presented in Figs. 9–11.

According to both of the experimental and the model curves in these figures, As^{5+} is the weakest

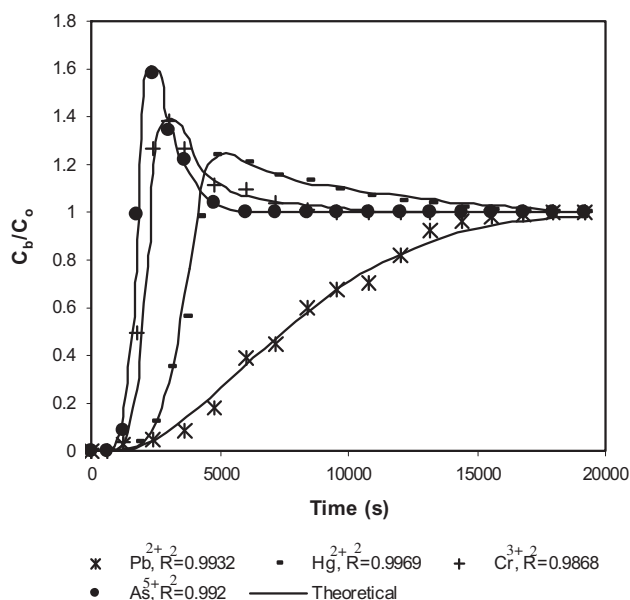


Fig. 11. Breakthrough curve for biosorption of heavy metals onto DAS in quaternary system, Pb^{2+} - Hg^{2+} - Cr^{3+} - As^{5+} . $C_o = 50 \text{ mg/L}$ each metal cations.

adsorbed component and Pb^{2+} is the strongest adsorbed component since the breakpoint of arsenic cations is the lowest value followed by chromium, mercury, and lead in binary, ternary, and quaternary systems. This sequence corresponds to the sequence of increasing affinity of these metals towards the biosorbent. This is in agreement with the results of [31,32].

At the initial stage, there are a lot of active sites on activated sludge. These sites are remained vacant till the molecules of the components are presented in the solution. The stronger and weaker adsorbed components take the active sites freely. With increasing time, the weaker adsorbed component is not easily adsorbed but moves away with the bulk fluid. Because the stronger adsorbed components tend to take the active sites instead of the weaker adsorbed component, it will displace the sites that had been occupied by the weaker adsorbed components. The result is that the local concentration of the weaker adsorbed component within the fixed-bed adsorber is higher forming an overshoot. The predictions concerning the magnitude of the overshoots of Hg^{2+} , Cr^{3+} , and As^{5+} are in a good agreement with the experimental data. No overshoot was reported for the metal of high affinity, Pb^{2+} .

According to Kratochvil and Volesky [33], the key component in the wastewater is the toxic species whose concentration in the column effluent first exceeds the discharge limit set by regulations, thereby determining the service time of the column and hence also the biomass usage rate in the process. Thus, in present study, arsenic was considered the key component in quaternary system and the service time of the column was reported to be 951 s. For binary and ternary systems, the column service time was higher.

4. Conclusion

A wide range of batch and fixed-bed experiments were carried out covering four metals ions. The Langmuir isotherm model was well described the sorption process of single-component systems onto dried activated sludge. Extended Langmuir model was well fitted with the equilibrium isotherms for multicomponent systems. The maximum biosorption uptake of the studied metal ions in single, binary, ternary, and quaternary systems by activated sludge showed the following affinity order $\text{Pb}^{2+} > \text{Hg}^{2+} > \text{Cr}^{3+} > \text{As}^{5+}$. The biosorption capacity for single metal decreased by 11–51, 53–88, and 79–94% in the binary, ternary, and quaternary systems, respectively, at the optimum agitation speed 600 rpm. FTIR analysis showed that carboxylic acid, amide, and amine groups

played the most important role in binding lead, chromium, mercury, and arsenic cations onto DAS. Predictions model for the experimental breakthrough curves compared well.

When metals are gathered in mixtures as multicomponent systems, arsenic breakthrough curve appears from the column first with higher overshoot, followed by chromium, mercury, and finally lead cations with no overshoot. Minimum service time or biosorbent usage time of the fixed bed was found for the quaternary system. COMSOL software was proved to be an effective numerical tool to predict breakthrough curve for fixed-bed adsorber.

This study indicated that the activated sludge can be used as an effective and environmentally friendly adsorbent for the treatment of heavy metals containing wastewater.

Abbreviations

A	— cross-sectional area of the adsorber, m^2
b_i	— Langmuir constant, m^3/kg
C_{bi}	— concentration of solute i in the fluid phase of the column, kg/m^3
c_{bi}	— scaled concentration of solute i in the fluid phase of the column, C_{bi}/C_{oi}
C_e	— equilibrium concentration, mg/L
C_{oi}	— initial concentration of solute i , mg/L
C_{pi}	— concentration of solute i in the fluid phase within the pores of the biosorbent, kg/m^3
c_{pi}	— scaled concentration of solute i in the fluid phase within the pores of the biosorbent, C_{pi}/C_{oi}
D_L	— axial dispersion, m^2/s
D_{mi}	— molecular diffusion coefficient of component i , m^2/s
D_{pi}	— pore diffusion coefficient of component i , m^2/s
d_p	— particle diameter, m
k_{fi}	— external mass transfer coefficient of solute i , m/s
L	— bed height, m
P_e	— Peclet number, vL/D_L
Q	— flow rate, m^3/s
q_{mi}	— adsorption equilibrium constant defined by Langmuir equation of component i , kg/kg
R	— radial distance in the particle, m
R_e	— Reynolds number, $\left(\frac{\rho_w v d_p}{\mu_w}\right)$
R_p	— radius of particle, m
R_s	— separation factor, $\frac{1}{1 + b C_e}$
r	— scaled radial distance in the particle, R/R_p
Sc_i	— Schmidt number of component i , $\left(\frac{\mu_w}{\rho_w D_{mi}}\right)$
Sh_i	— Sherwood number of component i , $\left(\frac{k_f d_p}{D_{mi}}\right)$
V_L	— initial volume of solution, mL
V_f	— final volume of solution, mL

W	— mass of activated sludge biomass, g
t	— time, s

Greek symbols

ε_b	— bed porosity
ε_p	— particle porosity
v	— interstitial velocity $\left(\frac{Q}{A_{cb}}\right)$, (m/s)
ρ_p	— density of particle, kg/m^3
ρ_w	— density of water, kg/m^3
μ_w	— viscosity of water, $Pa \cdot s$

Subscripts

j	— integer value
L	— liquid phase
p	— pore phase

References

- [1] R.W. Bayrak, Coast and marine de-pollution by adsorption, Dissertation, University of Baghdad, 2006.
- [2] R.S. Dobson, J.E. Burgess, Biological treatment of precious metal refinery wastewater: A review, *Minerals Eng.* 20 (6) (2007) 519–532.
- [3] Z. Aksu, Application of biosorption for the removal of organic pollutants: A review, *Process Biochem.* 40 (11) (2005) 997–1026.
- [4] E. Kusvuran, D. Yildirim, A. Samil, O. Gulnaz, A study: Removal of Cu(II), Cd(II), and Pb(II) ions from real industrial water and contaminated water using activated sludge biomass, *Clean Soil, Air, Water* 40 (11) (2012) 1273–1283.
- [5] L. Ping, X. Guohua, Competitive adsorption of phenolic compounds onto activated carbon fibers in fixed bed, *J. Environ. Eng.* 127 (August 2001) 730–734.
- [6] G. Belfort, Adsorption on carbon: Theoretical considerations, *Environ. Sci. Technol.* 14 (8) (1980) 910–913.
- [7] P.M. Alexander, Adsorption isotherms analysis, *J. Environ. Eng.* 221 (3) (2002) 60–63.
- [8] C.Z. Kannan, Multi-component model adsorption kinetics, *Ch. Eng.* 4 (2001) 45–47.
- [9] COMSOL Inc., Chemical Engineering Module: Model Library, Version 3.5a, Burlington, (2008) 613–620.
- [10] X.J. Wang, S.Q. Xia, L. Chen, J.F. Zhao, J.M. Chovelon, J.R. Nicole, Biosorption of cadmium(II) and lead(II) ions from aqueous solutions onto dried activated sludge, *J. Environ. Sci.* 18 (5) (2006) 840–844.
- [11] B.M. Cocero, Modeling and prediction of specific compounds adsorption by activated carbon and synthetic adsorbents, *Water Res.* 14 (2004) 1719–1728.
- [12] A.J. Jayson, Dubinin-isotherm application in adsorption, *ASCE Env. J.* 10 (2000) 70–79.
- [13] F.T. Batt, The Theory of Adsorption and Catalysis, Academic press, London, 1997.
- [14] A.R. Khan, T.A. Al-Bahri, A.A. Al-Haddad, Adsorption of phenol based organic pollutants on activated carbon from multi-component dilute aqueous solutions, *Water Res.* 31 (1997) 2102–2112.
- [15] R. Sips, On the structure of a catalyst surface, *J. Chem. Phys.* 16 (1984) 490–495.

- [16] A.H. Sulaymon, K. Ahmed, Removal of lead, cadmium, and mercury ions using biosorption, *Desalin. Water Treat.* 24 (2010) 344–352.
- [17] A.H. Ali, Performance of adsorption/biosorption for removal of organic and inorganic pollutants, Dissertation, University of Baghdad, 2011.
- [18] A.H. Sulaymon, S.E. Ebrahim, M.J. Mohammed-Ridha, Equilibrium, kinetic, and thermodynamic biosorption of Pb(II), Cr(III), and Cd(II) ions by dead anaerobic biomass from synthetic wastewater, *Environ. Sci. Pollut. Res.* 20 (2013) 175–187.
- [19] A.J. Garden, Application of Harkins model in adsorption, *J. Int. Assoc. Hydrologists* 7 (2006) 11–14.
- [20] D.M. Ruthven, *Principle of Adsorption and Adsorption process*, Wiley, New York, NY, 1984.
- [21] L. Yao, Z.F. Ye, Z.Y. Wang, J.R. Ni, Characteristics of Pb²⁺ biosorption with aerobic granular biomass, *Chin. Sci. Bull.* 53 (2008) 948–953.
- [22] S.A. Onga, E. Toorisakaa, M. Hirataa, T. Hanoa, Adsorption and toxicity of heavy metals on activated sludge, *Sci. Asia* 36 (2010) 204–209.
- [23] A.H. Sulaymon, B.A. Abid, J.A. Al-Najar, Removal of lead copper chromium and cobalt ions onto granular activated carbon in batch and fixed-bed adsorbers, *Chem. Eng. J.* 155 (2009) 647–653.
- [24] J.U. Oubagaranadin, J.V. Murthy, B.S. Rao, Applicability of three-parameter isotherm models for the adsorption of mercury on fuller's earth and activated carbon, *Indian Chem. Eng.* 49 (3) (2007) 196–204.
- [25] L. Rajaković, The sorption of arsenic onto activated carbon impregnated with metallic silver and copper, *Sep. Sci. Technol.* 27 (11) (1992) 1423–1433.
- [26] H.M. Abdul-Hameed, Competitive adsorption of heavy metals onto activated carbon in fixed bed column, Dissertation, University of Baghdad, (2009).
- [27] A. Fahmi, K. Munther, Competitive adsorption of nickel and cadmium on sheep manure waste, experimental and prediction studies, *Sep. Sci. Technol.* 38 (2003) 483–497.
- [28] S.A. Yousif, A.H. Sulaymon, M.M. Alfaize, Experimental and theoretical investigations of lead mercury chromium and arsenic biosorption onto dry activated sludge from wastewater, *Int. Rev. Chem. Eng.* 5 (1) (2013) 30–40.
- [29] P. Gupta, A. Nanoti, M.O. Garg, The removal of furfural from water by adsorption with polymeric resins, *Sep. Sci. Technol.* 36 (13) (2001) 2835–2844.
- [30] D.W. Hand, J.C. Crittenden, W.E. Thacker, User-oriented batch reactor solutions to the homogeneous surface diffusion model, *J. Environ. Eng.* 109 (1) (1983) 82–101.
- [31] A. Bakir, Development of a seaweed-based fixed-bed sorption column for the removal of metals in a waste stream, Dissertation, Waterford Institute of Technology, 2010.
- [32] G. Naja, B. Volesky, Multi-metal biosorption in a fixed-bed flow-through column, *Colloids Surf., A* 281 (2006) 194–201.
- [33] D. Kratochvil, B. Volesky, Multicomponent biosorption in fixed beds, *Water Res.* 34 (12) (2000) 3186–3196.